CERN - European Laboratory for Particle Physics

INFN - Istituto Nazionale di Fisica Nucleare

CERN-SL/99-034(DI)
INFN/AE-99/05

The CERN Neutrino beam to Gran Sasso (NGS)

Addendum to report CERN 98-02, INFN/AE-98/05

R. Bailey, J. L. Baldy, A.E. Ball, P. Bonnal, M. Buhler-Broglin, C. Détraz, K. Elsener (Ed.), A. Ereditato, P. Faugeras, A. Ferrari, G. Fortuna, A. L. Grant, A. Guglielmi, A. Hilaire, K. Hübner, M. Jonker, K. H. Kissler, L.A. Lopez-Hernandez, J.M. Maugain, P. Migliozzi, V. Palladino, F. Pietropaolo, J.P. Revol, P. Sala, C. Sanelli, G. R. Stevenson, N. Vassilopoulos, H. Vincke, E. Weisse, M. Wilhelmsson

Abstract

The conceptual technical design of the NGS (CERN neutrino beam to Gran Sasso) facility has been presented in the report CERN 98-02 / INFN-AE/98-05. Additional information, in particular an update on various neutrino beam options for the NGS facility, has been provided in a memorandum to the CERN-SPSC Committee (CERN-SPSC/98-35). In the present report, further improvements on the NGS design and performance, in particular new scenarios for SPS proton cycles for NGS operation and a new version of the NGS 'high-energy' neutrino beam for ν_τ appearance experiments, are described. This new NGS reference beam is estimated to provide three times more ν_τ events per year than the beam presented in the 1998 report. The radiological aspects of the NGS facility have been re-examined with the new beam design. An updated version of the construction schedule is also presented.

Contents

1 Introduction

The Super-Kamiokande results on the atmospheric ν_μ deficit and azimuthal dependence [1], which can be interpreted as being due to neutrino oscillation (with a larger probability for the channels $\nu_\mu - \nu_\tau$ or $\nu_\mu - \nu_{sterile}$) gave an additional boost to the world-wide interest in accelerator long-baseline oscillation experiments.

In Europe, the focus is on a ν_μ beam for ν_τ appearance, produced by protons from the CERN-SPS, directed towards the Gran Sasso laboratory (LNGS) in Italy, 732 km away from CERN. The design and performance of the CERN neutrino beam to Gran Sasso - the NGS facility - are described in a conceptual technical design report [2]. This design has since been scrutinized and improved, and options for appearance and disappearance experiments have been investigated. The updated design variants, including high and low energy ν_μ beams and a new estimate of the available protons on target per year, have been presented to a joint meeting of CERN's SPS Scientific Committee (SPSC) and the Gran Sasso Scientific Committee (LNGSC) on 3 November 1998. The beam spectra and performances available at that time have been summarized in a memorandum to the SPSC [3]. On the same occasion, the proponents of various long base-line experiments submitted letters of intent, describing the physics potential of their ideas. That SPSC/LNGSC meeting concluded [4] that the Super-Kamiokande result *'calls for a combined experimental programme with the following goals:'*

- ... (a new, massive atmospheric neutrino experiment at Gran Sasso)
- *'A precise test of the $\nu_\mu - \nu_\tau$ oscillation hypothesis with an experiment utilizing the Neutrino beam to Gran Sasso (NGS) as laid out in [2, 3]. The feasibility of constructing such a neutrino beam has been demonstrated. The underground experiment would be able to determine the $\nu_\mu - \nu_\tau$ oscillation hypothesis in the mass region above 1 to 2×10^{-3} eV^2. Ways of extending this mass range may exist by using a detector on the surface. The search for ν_e appearance may also be coupled with ν_τ appearance experiments.*'

With these guidelines, the NGS beam has been optimized for ν_τ appearance experiments at Gran Sasso. The main changes are:

- an increased average proton current during fixed-target operation by a more optimal use of the SPS
- the impact on the number of protons for NGS due to the parallel running of LHC and NGS
- an increased rate of ν_τ CC events per proton on target by
  - changing the secondary beam optics to improve the acceptance and to optimise the shape of the spectrum, in order to match the oscillation probability for the Δm^2 range indicated by Super-Kamiokande
  - increasing the current in the co-axial lenses (horn and reflector)
  - reducing the amount of material in the secondary beam (pions, kaons).

The result is an expected increase of about a factor three in the number of charged current ν_τ events per year at Gran Sasso, when compared to the initial design [2]. The present addendum to the 1998 report describes the new developments and provides an updated construction schedule for the NGS facility. This new schedule foresees start of operation in the first half of 2005 provided that a positive decision is taken no later than at the end of 1999.

The cost estimate of 71 MCHF for the NGS, presented in [2], has not changed. It should be pointed out, however, that this is the marginal cost of NGS. NGS can largely profit from investment for LHC - this is estimated to represent a value of 15 MCHF, not included in the NGS cost quoted above. Furthermore, equipment worth about 7 MCHF will be recuperated for the NGS from various installations at CERN, in particular from the WANF and LEP [5]. Hence, the true cost of NGS is 93MCHF.

2 Proton beam

In order to explore the full potential of the NGS long-baseline experiments, a maximum number of protons on NGS target (pot) per year is required. The SPS limitations and NGS target constraints have to be taken into account. For a realistic scenario of SPS operation, the impact from LHC operation as well as the requests for slow extracted (SE) beam for the fixed-target physics community and test beam users have to be anticipated.

The boundary conditions for SPS running were carefully studied. After publication of the NGS report [2], it was found that the RF acceleration programme could be shortened by 0.2 s. This allows to reduce the length of NGS cycles with two fast extractions at 400 GeV/c from 6.2 to 6.0 s. The gain for NGS is much more striking: a rhythm of 1.2 s is imposed by the PS injector complex, hence the SPS cycle time for NGS is reduced from 7.2 s [2] to 6.0 s. This has a considerable impact on the pot/year for NGS.

Since the energy of the proton beam for the slow extraction users is to be restricted to 400 GeV/c in the future for budgetary reasons, the power dissipation in the SPS magnets is no longer a relevant limitation and longer supercycles leading to larger numbers of pot/year for NGS can be envisaged. On the other hand, the running-in and operation of the LHC will have an impact on the SPS availability for NGS and other fixed target users. Taking all these factors into account, the expected number of protons on the NGS target is

$$4.5 \times 10^{19} \text{ pot/year}$$

when operating in parallel with LHC. In order to provide an idea of the reduction in performance by sharing time with LHC and protons with other fixed-target users, this number is compared with the upper limit, namely the performance in dedicated operation which would provide 7.6×10^{19} pot/year assuming 200 days of operation per year. This indicates a significant but unavoidable loss (40 %) due to sharing. Details are described in the following sections.

2.1 SPS operation in the past years

The length of typical SPS runs, the maximum intensity achieved per cycle as well as the overall efficiency (protons delivered on target vs. protons expected) is well documented. For the year 1997 [6], for example, there was a peak intensity of 4.8×10^{13} per cycle, and for a scheduled run of 137 days of proton running a total number of 2.2×10^{19} protons, implying that an efficiency of 55% has been achieved. This efficiency includes downtimes as well as non-optimal operation periods of the machines in the proton acceleration chain at CERN.

Therefore, it is considered realistic to assume future SPS running with the already achieved performances, i.e. peak intensity of 4.8×10^{13} protons per cycle with an overall efficiency of 55%.

2.2 Operation modes of the SPS

When LHC is filled and the beams are coasting, the SPS is available for fixed-target physics. Two modes are possible: i) the shared mode where NGS and other fixed-target users get protons from different cycles within one supercycle; ii) the dedicated mode where NGS gets all the protons.

Once LHC is getting towards the end of a coast which is estimated to last about ten hours [7], the injector chain and the transfer lines are being set up with low-intensity pilot beams, which may take hours, in particular in the first years of LHC operation. In order not to disrupt completely NGS operation, it is proposed to interleave the LHC pilot cycle with NGS cycles in one supercycle. When it comes to the actual filling of LHC, the injector chain is fully dedicated to LHC and both rings are filled in 8 min in total.

Further examination may reveal that switching from the interleaved supercycle to the dedicated LHC cycle does not provide the required reproducibility, and that it might be better to work always with a supercycle comprising the LHC fill cycle plus the NGS cycles. This would lengthen the LHC fill by about a factor two but would provide very stable conditions.

Since the real filling of LHC takes only a few times a quarter of an hour or less per day its impact on NGS is negligible, independent of the choice of the supercycle for the LHC fill. Also the choice of the interleaved supercycle for the pilot pulses has little effect on NGS - both of these supercycles provide nearly the same average proton current to NGS. Hence, no immediate decision has to be taken, leaving time for a thorough study of the two alternatives. In all cases, it is indispensable that the SPS control system be modified allowing for rapid and reproducible switching between supercycles. It is planned to implement this feature by 2003 for the first LHC injection tests [8]. The PS complex was upgraded in this respect a few years ago.

In order to make an estimate of the expected pot/year for NGS, assumptions on the SPS supercycles have to be made and a scenario of a possible symbiosis between LHC operation and SPS fixed-target physics has to be conceived.

For comparison of the average proton current provided by these various cycles, the number of protons on target is given which would be obtained if one used the considered cycle exclusively for 200 days. This number of days is chosen as it is close to the scheduled duration of the physics runs with protons and ions in the last ten years (as a matter of fact, about 190 days

were often reached with a record of 217 days in 1998 [6]).

Protons are injected into the SPS from the PS, operating at a cycle time of 1.2 s. Therefore, SPS operation has to follow this 'clock', i.e. any SPS supercycle has to be a multiple of 1.2 s. Typically, two PS injections per SPS cycle are used (as is the case in the present SPS operation for fixed target proton physics). This is the basis for all the supercycles presented below.

Injecting three pulses from the PS and extracting three pulses for NGS would increase the average proton current per NGS cycle by only 25%. The target limit which is around 2.4×10^{13} protons per pulse would be respected. However, the presently known beam stability limits in the SPS would be exceeded resulting in intolerable beam loss and low transmission. Furthermore, the injection of three pulses has been tried out in machine development runs without positive results. Further studies are needed to understand these limitations. For all these reasons, only the injection of two PS pulses is considered further.

2.2.1 Expected protons on target in shared operation

While the beams are coasting in LHC, various scenarios can be imagined for an SPS operation serving NGS as well as other users who are typically requiring a slow extracted beam on target. It can be anticipated that a certain amount of test beam time will be required in 2005 and beyond, particularly by the LHC experiments, but also for R&D or fixed target experiments. For budgetary reasons, the present policy of CERN foresees to run the SPS at 400 GeV/c (or lower) from 2002 onwards [9]. This is taken as a basis assumption for the following considerations. It has been shown [10] that this allows various SPS supercycles with 2, 3 or 4 NGS cycles, all of which respect the power dissipation limits given for the SPS magnets. Table 1 gives a (non-exhaustive) list of possible SPS supercycles for shared operation between NGS and SE users.

As an example, the supercycle with 27.6 s duration (cf. Fig. 1) is considered to be the nominal one throughout this report. It provides a relatively high average proton current for NGS leading to 5×10^{19} pot/year with a reasonable length of the supercycle and a duty cycle of the slow extraction of 13% (to be compared to 16% in present operation and for the nominal shared supercycle assumed in ref. [2]).

Table 1: *SPS shared operation, assuming 400 GeV/c pot for all users (from [10]).*

Number of NGS cycles per supercycle	supercycle T_{sc} [s]	slow extraction T_{FT} [s]	NGS pot/year [10^{19} / 200 d]
2	21.6	3.5	4.22
2	22.8	4.7	4.00
3	27.6	3.5	4.96
3	28.8	4.7	4.75
4	33.6	3.5	5.43
4	34.8	4.7	5.24

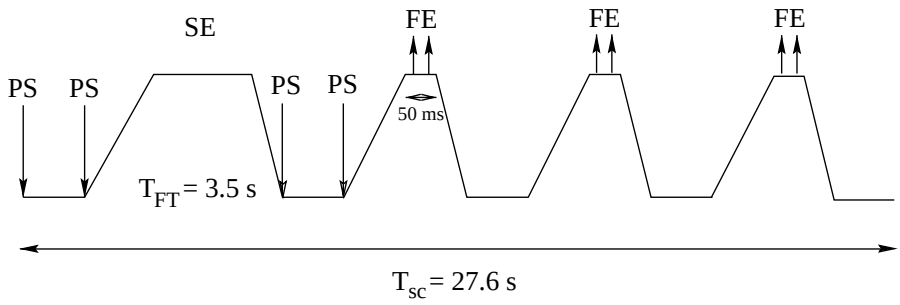

Figure 1: *Schematic view of a possible SPS supercycle for shared operation. A 3.5 s flat-top for slow extraction (SE) at 400 GeV/c is followed by three NGS cycles, also at 400 GeV/c.*

2.2.2 Expected protons on target in dedicated operation

A close look at the time needed for an NGS cycle with two fast extractions at 400 GeV/c shows that 6.0 s are sufficient. With this shortened cycle time (cf. Fig. 2), and using the SPS intensity per cycle and efficiency as mentioned above, one finds that 7.6×10^{19} pot/year can be achieved for NGS in 200 days of dedicated operation. This gives the upper performance limit.

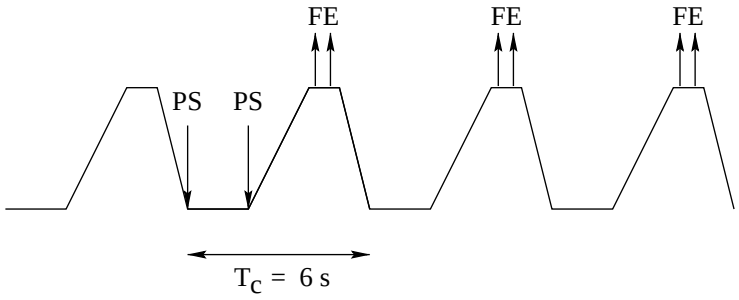

Figure 2: *Schematic view of SPS cycles for dedicated NGS running at 400 GeV/c.*

2.2.3 Supercycle with interleaved LHC pilot cycle and NGS cycles

A low-intensity pilot beam consisting of only one bunch will be used for setting-up the injector chain of LHC, the transfer lines, injection into LHC, and the energy ramping in LHC. Fig. 3 shows an example of such a cycle combined with 2 cycles for NGS.

2.2.4 Supercycle with interleaved LHC cycle and NGS cycles

Once all the adjustments for LHC are made using the supercycle with the pilot cycle, LHC can be filled with a dedicated cycle within somewhat less than 4 min for each of the counter-rotating beams. However, this introduces the risk that the settings are influenced by this change in supercycle and that the injected beam does not fulfill the stringent requirements of LHC, though filling is very rapid and the risk of drifts, especially due the persistent currents in the LHC superconducting magnets, is minimized.

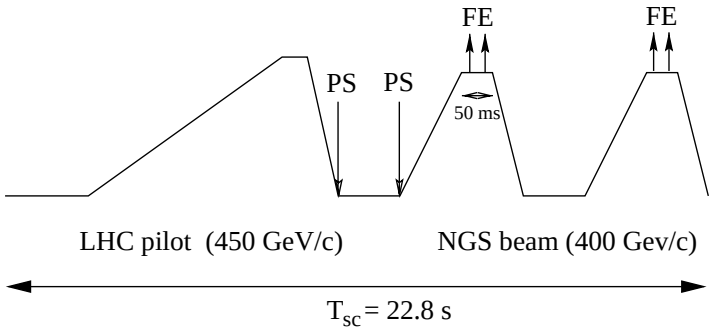

Figure 3: *Schematic view of a possible SPS supercycle with interleaved LHC pilot cycle at 450 GV/c and NGS cycles at 400 GeV/c.*

Another strategy would be to use the same supercycle for the pilot beams and the LHC filling. An example of such a supercycle is shown in Fig. 4 below. The drawback of this supercycle is its length making observations and tuning a bit more tedious as well as doubling the actual filling time of LHC. However, it provides maximum reproducibility between setting-up with pilot beams and filling. There is no strong reason for choosing three NGS cycles, eventually two or four NGS cycles might be chosen.

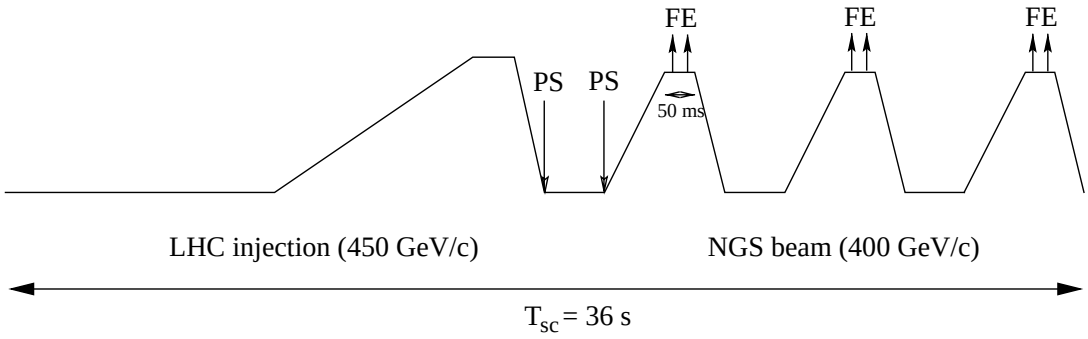

Figure 4: *Schematic view of a possible SPS supercycle with interleaved LHC filling cycle at 450 GeV/c and NGS cycles at 400 GeV/c.*

2.3 Expected number of protons on target per year

Table 2 gives the average proton currents for NGS for the four examples of supercycles expressed in terms of pot in 200 days.

In order to estimate the effective pot/year, a model of the operation of LHC from 2005 onwards is required. It seems to be appropriate to distinguish between the year 2005 where the

Table 2: *Average proton current for NGS.*

Supercycle	T_{sc} [s]	NGS [10^{19} pot / 200 d]
Shared SE / NGS	27.6	5.0
Dedicated NGS	6.0	7.6
Interleaved LHC pilot / NGS	22.8	4.1
Interleaved LHC fill / NGS	36.0	3.9

running-in of LHC will start in July, and the following years when LHC is running though a considerable fraction of the time is still spent on improving its performance.

2.3.1 Operation in 2005

The following scenario is proposed as example assuming that LHC will be commissioned and have its first physics runs with protons in July to October:

March-April:	NGS commissioning with shared SE/NGS supercycle	
May-June:	shared SE/NGS	
July-August:	50% LHC commissioning, 50% shared SE/NGS	
September-October:	for 3/4 of the week per day:	2×4 h interleaved LHC pilot/NGS
		16 h shared SE/NGS
	for 1/4 of the week:	LHC machine development with
		interleaved LHC/NGS supercycles.
November:	50% LHC commissioning with ions, 50% shared SE/NGS.	

Note that the LHC filling is neglected since it takes each time only a small fraction of an hour. Also choosing the other interleaved supercycle (see 2.2.4) instead of the one described under 2.2.3 for the setting-up of LHC will not change the result as their average proton currents are virtually the same (cf. Table 2).

Table 3 gives the expected pot/year for NGS and for the users of the slow-extraction (SE) for different possible schedules. The first line illustrates the impact of LHC which would reduce the pot/year to 72% of the value expected for shared operation without LHC. The other lines demonstrate that a number of scheduling options exist to nearly or completely reach the pot/year expected from unperturbed shared operation for 200 days. Thus, it seems reasonable to assume that 4.5×10^{19} pot can be achieved for the NGS facility in 2005.

The total number of protons for SE was calculated assuming, as for NGS, 4.8×10^{13} protons per SE cycle and an efficiency of 55%. The result is best put into perspective by comparing it with the requirements of COMPASS in phase I (0.4×10^{19} per year) [11] and the present number of protons on target for detector tests in the North and West halls (0.14×10^{19} in 1998) [6]. Obviously, the approved phase I of COMPASS will be terminated by 2005 but comparison shows that there will be no lack of protons either for phase II of COMPASS or other new fixed-target experiments.

Table 3: *Expected pot/year in 2005 for NGS and SE for various scheduling options.*

May-Oct.	Add Nov.	May/June no SE	July no SE	NGS 10^{19} pot / year	SE 10^{19} pot / year
x				3.6	1.5
x	x			4.0	1.6
x		x		4.4	1.0
x	x	x		4.7	1.1
x	x	x	x	5.2	1.0

2.3.2 Operation after 2005

A possible scenario is that LHC operates with protons in April to October with the same sharing between LHC, NGS and SE as in September and October 2005. One may argue that the machine development time will decrease in later years leading to some increase of availability for NGS. On the other hand, the steadily growing LHC luminosity will reduce the length of the LHC coast requiring more frequent LHC filling. To first order, the same conditions will prevail as in 2006.

Table 4 shows that a fairly good performance can be expected for the fixed-target programme. Two options are also shown to indicate the flexibility in the scheduling. The first option is to continue proton-fixed target operation in November using the time when LHC is filled with ions and the beams are coasting. It is assumed that 50% of the time is available for proton fixed-target operation and the SPS operates with the supercycle sharing protons between SE and NGS (see 2.2.1). The other option shown in the third line assumes that for 40 days all the time when LHC has coasting proton beams is dedicated to NGS.

Since our model of operation in the years after 2005 is rather crude and not all implications of the interleaved cycles for LHC performance have been studied thoroughly, it seems to be prudent to assume as nominal performance not being the maximum offered by the options but only 90% leading to 4.5×10^{19} pot/year for NGS. Concerning the pot/year available for SE users, the same comments as for 2005 apply.

Table 4: *Expected pot/year after 2005 for NGS and SE for various scheduling options.*

April-Oct.	Add Nov.	no SE for 40 d	NGS 10^{19} pot/year	SE 10^{19} pot/year
x			4.7	0.87
x	x		5.1	1.0
x		x	5.0	0.70

3 An improved ν_μ beam for ν_τ appearance experiments

3.1 Remarks on the 1998 NGS reference beam

The beam presented in the NGS report [2] provided a stable framework on which to base the detailed studies of the civil engineering, infrastructure and radiological issues. The NGS has to be considered as a long-term facility: choosing the parameters of a high energy, wide-band beam as a 'reference' ensured that a wide range of possible beam variants could be accomodated within the established civil engineering constraints. The high energy design was based on previous beams in the WANF and used similar material thicknesses and pulsed currents. The design was also significantly influenced by the requirements for a short-baseline facility.

The more specific design goal for the new beam, i.e. optimisation for long-baseline ν_τ appearance, has led to a revised beam optics layout to maximize the secondary beam acceptance in the desired momentum range. At the same time, modern construction methods for the magnetic horns will lead to much reduced material in the beam aperture.

3.2 Conditions for optimum ν_τ appearance

The criterion for ν_μ - ν_τ appearance experiments is the number of observable ν_τ charged current (CC) events. According to the latest results from the Super-Kamiokande experiment [1], the neutrino mass difference Δm^2 where such an oscillation is thought to occur is in the range of 10^{-3} to 10^{-2} eV^2 for full mixing. The rate of ν_τ CC events [1] from the ν_μ beam is given by:

$$R_\tau = A \int \phi_{\nu_\mu}(E) \times P_{osc}(E) \times \sigma_\tau(E) \times \epsilon(E) \times \mathrm{d}E$$

where A is the number of nucleons in the effective detector mass, $\phi_{\nu_\mu}(E)$ is the ν_μ fluence at Gran Sasso, $\epsilon(E)$ represents the (detector-dependent) detection efficiency of the ν_τ events, $\sigma_\tau(E)$ is the ν_τ CC cross section and P_{osc}, the oscillation probability. For two flavour mixing, the latter can be expressed as

$$P_{osc} = \sin^2(2\theta) \times \sin^2(1.27 \times \Delta m^2 \times L \,/\, E).$$

Neglecting the detection efficiency $\epsilon(E)$, the neutrino spectrum $\phi_{\nu_\mu}(E)$ should match the product $P_{osc} \times \sigma_\tau(E)$. For the values Δm^2 of interest here the neutrino energy E at which this product has a maximum hardly depends on the neutrino mass difference.

Whilst the cross sections for ν_μ CC events compare well with experimental data at high energy, there is still a considerable uncertainty in the cross sections for ν_τ, in particular in the region near the τ production threshold. In the following evaluations of CC event rates, the cross section tables given on the NGS WWW page [12] are used.

[1] Note that, in general, we refer to CC events as the total probability for charged current interactions, i.e. the sum of deep inelastic, quasi elastic and resonance contributions.

3.3 The new NGS reference beam

Compared to the 1998 report [2], the civil engineering design of the NGS facility remains unchanged. Optimizing the probability for ν_τ appearance at Gran Sasso implies maximizing the ν_μ fluence in the range of 10 to 30 GeV. The horn and the reflector are therefore designed to focus 35 GeV and 50 GeV secondary particles. In order to achieve a much higher acceptance at these energies, the two lenses are much closer to the target than in the 1998 beam. A schematic overview of the new NGS reference beam for appearance experiments is shown in Fig. 5. Note that the target cavern is longer than required for the new beam, in view of a possible future installation of a higher energy or narrow-band neutrino beam.

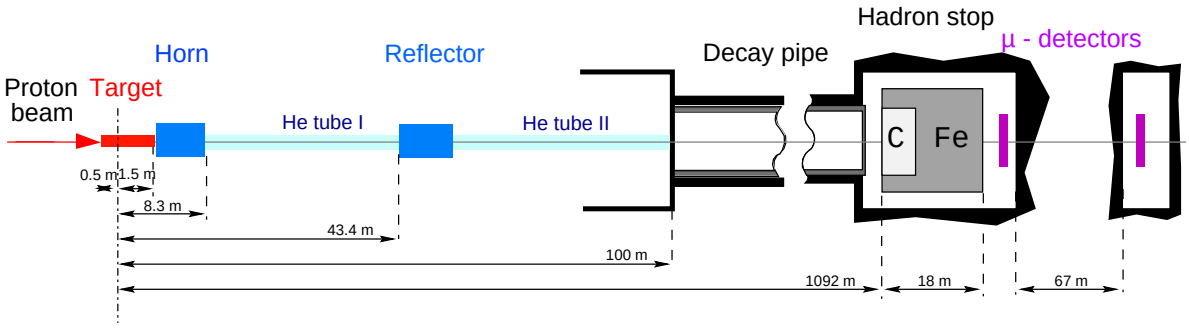

Figure 5: *Schematic overview showing the components of the new NGS reference beam. The coordinate origin is the focus of the proton beam.*

In the compact new design the target box position and dimensions remain unchanged. Additional graphite rods are added, while keeping the overall target length at 2 m. The target rod diameter has been increased from 3 mm to 4 mm so that the proton beam is better contained within the target: this reduces spurious background from residual protons interacting later in the beam line, without significant change to the ν_μ flux and energy spectrum. The thermo-mechanical properties of the target rods under shock from the proton beam impact is slightly improved by the increased rod diameter.

The first coaxial lens, the horn, now starts at 1.7 m from the focal point of the system, just after the end of the target, and the reflector is also moved upstream, to 43.4 m. With these changes, and using a higher current in the horn and the reflector (150 kA instead of 120 kA), the nominal acceptance for pions and kaons between 20-50 GeV has been increased by 50%.

Prototype tests have demonstrated the feasibility of using electron beam welding to assemble the inner conductor elements, rather than the bolted flanges previously used. Many details of the horn and reflector construction have been re-examined. Apart from a small, local increase in the horn inner conductor thickness because of the higher current, the net result is a significant reduction of the total amount of material within the beam aperture.

Similarly to the 1998 design, helium tubes are foreseen in the free spaces of the target chamber in order to reduce the interaction probability for the secondary hadrons. In the new layout, a first He tube is located between the horn and reflector, while a second one fills the gap

between the reflector and the decay tunnel.

In order to move the horn close to the target, the collimators installed after the target in the 1998 NGS beam have been removed. A more general shielding around the target, horn and helium tubes is now used. An overview of the target cavern layout can be found in Fig. 6 with a more detailed view of the target/horn region shown in Fig. 7.

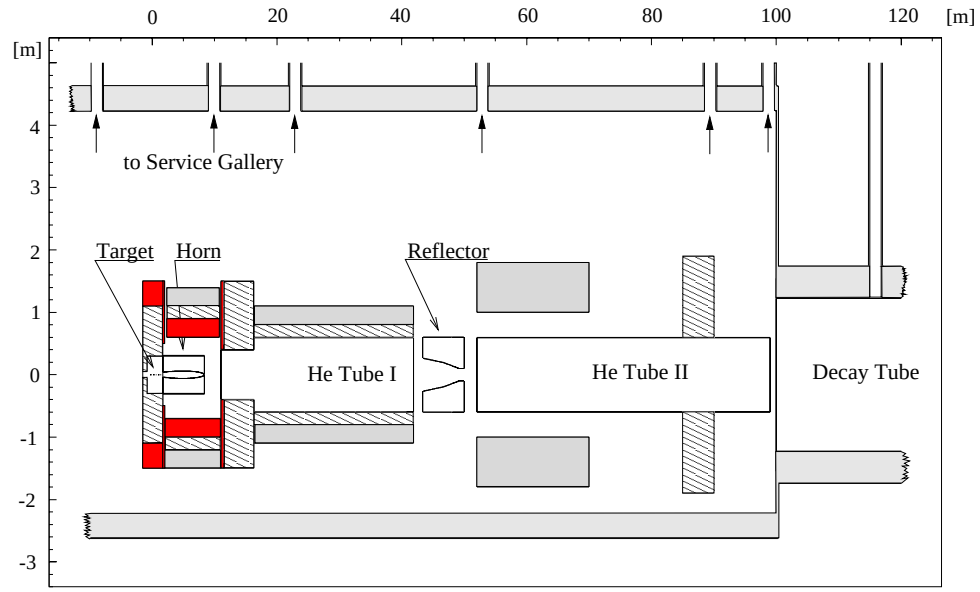

Figure 6: *The layout of the new NGS reference beam. (Note that, in order to make the important items of the beam more visible, the scale on the two axes is very different).*

The parameter list for the new NGS reference beam is given in Appendix A. Three-dimensional views into the target chamber, with all components of the shielding, are presented in Appendix B. Further details on the design of the conductors in horn and reflector can be found in Appendix C, together with an updated table of their electrical characteristics. A description of the material used in the beam simulations is given in Appendix D.

3.3.1 ν_μ Performance

Two independent simulations were performed for transport and decay of the secondary particles. In one approach, hadron spectra from the 400 GeV/c protons impinging on the graphite target are generated by the FLUKA98 programme [13], and GEANT3.21 [14] is used for the transport and decay of the particles emerging from the target. The other approach is a FLUKA98 stand-alone simulation, starting from protons on target and ending with neutrinos at Gran-Sasso. There is good agreement between the two simulations.

The resulting NGS beam performance for the new reference beam is summarized in Table 5. The values given for the ν_μ beam have been obtained by averaging over a hypothetical detector

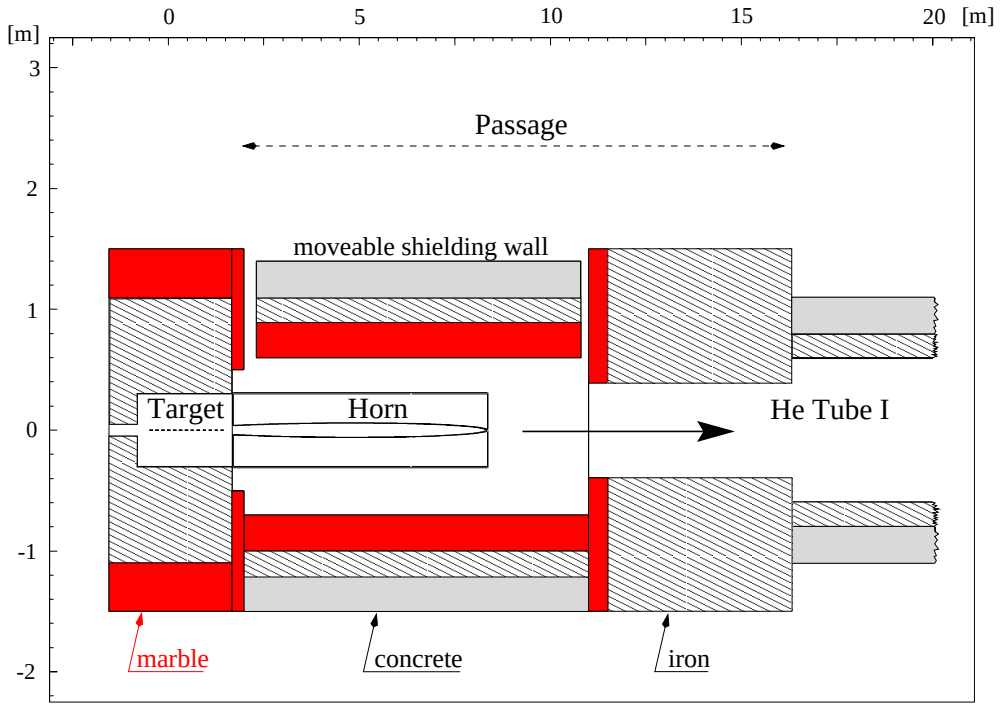

Figure 7: *Close-up on the region around target and horn.*

with radius 100 m at Gran Sasso[2]. In order to get reasonable statistical accuracy, this radius has been set to 400 m for ν_e, $\overline{\nu}_e$ and $\overline{\nu}_\mu$.

The expected numbers of detectable ν_τ for $sin^2 2\theta = 1$ and a few typical values of Δm^2 are shown in Table 6. When compared to the 1998 report [2], a substantial increase of about a factor of two in the expected ν_τ events per proton is found, This leads to an improved performance by a factor of three in ν_τ per kiloton and per year, taking into account that the estimated number of protons on target has increased from 3.0×10^{19} to 4.5×10^{19} per year.

The ν_μ fluence and expected CC event spectra at Gran Sasso are shown in Fig. 8. Fig. 9 shows a comparison with a hypothetical perfect beam of the same nominal acceptance: no absorption, and parent particles of all energies focused parallel to the beam axis.

The appropriate matching of the new NGS reference beam with the function $P_{osc}(E) \times \sigma_\tau(E)$ is demonstrated in Fig. 10. It should be pointed out that appearance experiments at Gran Sasso typically do not want the ν_μ spectrum to extend much beyond 30 GeV; as at higher energies, background channels open up which could be difficult to separate from the ν_τ events.

The more compact layout and larger angular acceptance for secondary particles from the target leads to a bigger diameter of the horn and reflector, thus to a beam with a larger diameter. It is therefore instructive to investigate the neutrino beam losses at Gran Sasso due to the limited diameter of the NGS decay tunnel. For the new NGS reference beam, the cumulative radial distribution of decaying hadrons which yield a neutrino at Gran Sasso is shown in Fig. 11. For

[2]The neutrino beam size at Gran Sasso is 1.37 km (rms. radius of the ν_μ CC event distribution).

Table 5: *Predicted performance of the new NGS reference beam. The statistical accuracy of the Monte-Carlo simulations is 1 % for the ν_μ component of the beam, somewhat larger for the other neutrino species.*

Energy region E_{ν_μ} [GeV]	1 - 30	1 - 100
ν_μ [m^{-2}/pot]	7.1×10^{-9}	7.45×10^{-9}
ν_μ CC events/pot/kt	4.70×10^{-17}	5.44×10^{-17}
$\langle E \rangle_{\nu_\mu\, fluence}$ [GeV]		17
fraction of other neutrino events:		
ν_e/ν_μ	0.8 %	
$\overline{\nu}_\mu/\nu_\mu$	2.0 %	
$\overline{\nu}_e/\nu_\mu$	0.05 %	

Table 6: *Expected number of ν_τ CC events at Gran Sasso per kt per year. Results of simulations for different values of Δm^2 and for $sin^2(2\theta)$ = 1 are given for 4.5 $\times$ 10^{19} pot/year. These event numbers do not take detector efficiencies into account.*

Energy region E_{ν_τ} [GeV]	1 - 30	1 - 100
$\Delta m^2 = 1 \times 10^{-3}$ eV^2	2.34	2.48
$\Delta m^2 = 3 \times 10^{-3}$ eV^2	20.7	21.4
$\Delta m^2 = 5 \times 10^{-3}$ eV^2	55.9	57.7
$\Delta m^2 = 1 \times 10^{-2}$ eV^2	195	202

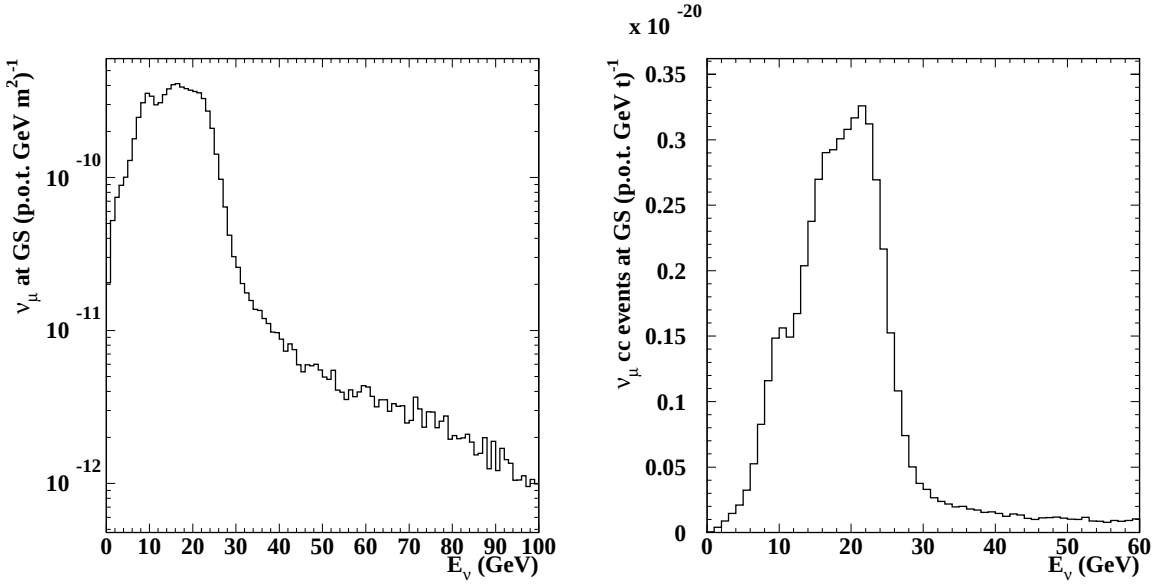

Figure 8: *Energy distribution of the ν_μ fluence (left) and of the CC ν_μ interactions (right) at Gran Sasso.*

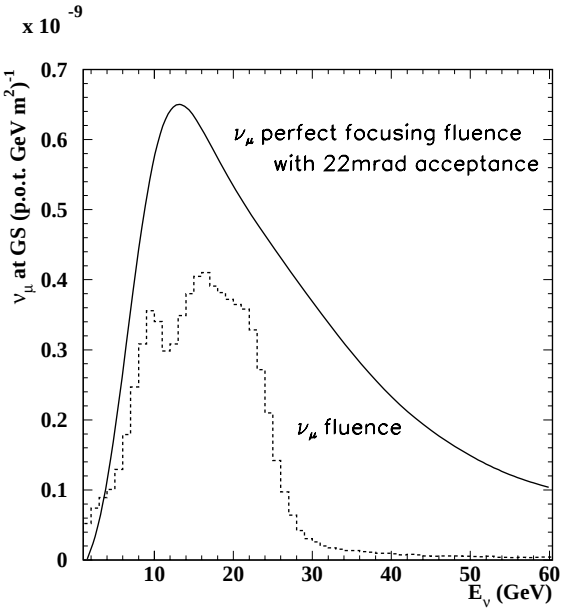

Figure 9: *Comparison of 'perfect focusing' with the ν_μ fluence at Gran Sasso.*

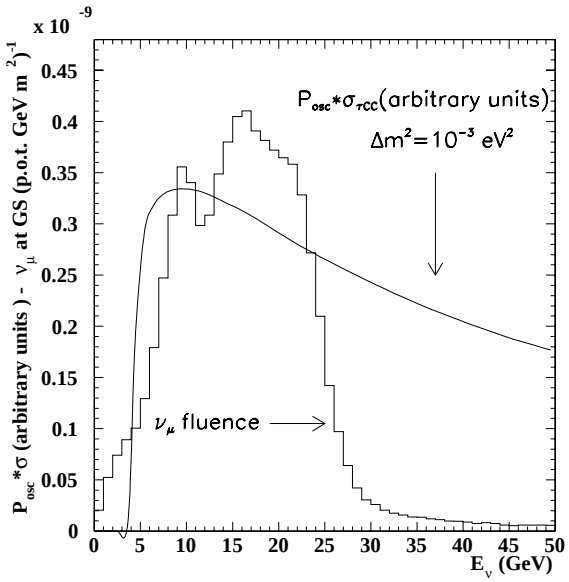

Figure 10: *ν_τ CC cross section times oscillation probability for small Δm^2 and full mixing, compared to the ν_μ fluence.*

completeness, the longitudinal distribution is also shown.

The fluence spectra for the beam contaminations in the new NGS reference beam can be found on the NGS WWW page [12], the fraction of background CC events (integrated up to 100 GeV/c) are given in Table 5. Note that tables with the numerical values of all spectra are also provided on the NGS WWW page.

3.3.2 A possible $\overline{\nu}_\mu$ beam

Even though the first goal of NGS is to perform a $\nu_\mu \rightarrow \nu_\tau$ appearance search, the availability of such a facility will offer other very interesting possibilities, for instance in the comparison between neutrino and antineutrino beams.

In the case of vacuum oscillations, the combined study of oscillations of neutrinos and antineutrinos could, in principle, allow the detection of possible CP violation effects in the neutrino sector ($P(\nu_\alpha \rightarrow \nu_\beta) \neq P(\overline{\nu}_\alpha \rightarrow \overline{\nu}_\beta)$). However, these effects are expected to be very small, vanishing in the limit when two neutrinos are degenerate in mass.

Larger differences in the oscillation probability could stem from a C violating effect due to the presence of matter. In that case ν_e's and $\overline{\nu}_e$'s behave differently because matter is not made of an equal amount of electrons and positrons. In matter, resonance effects can occur with neutrinos if the hierarchy is as expected ($m_{\nu_\mu} > m_{\nu_e}$). If it were the opposite, then resonance in matter could only occur with antineutrinos. Matter effects are advocated to be at work in the MSW mechanism as a possible explanation for the solar neutrino problem.

In the general case, in which all three neutrino families mix to some extent, the probabilities for ν's and $\overline{\nu}$'s oscillation will definitively differ because of matter effects. This difference is

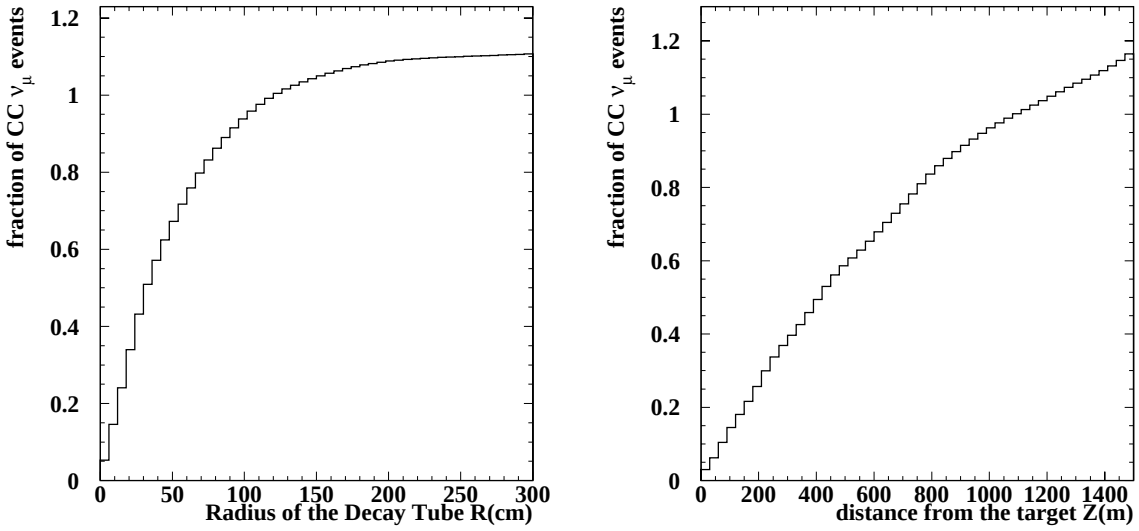

Figure 11: *Cumulative radial (left) and longitudinal (right) distribution of the decay points of parent hadrons which produce ν_μ events at Gran Sasso, normalised to the NGS design values R = 122.5 cm and Z = 1100 m.*

present even in the absence of CP–violating effects and could be detected at NGS [15, 16]. The study of the difference between $P(\nu_\mu \to \nu_e)$ and $P(\overline{\nu}_\mu \to \overline{\nu}_e)$ oscillations would allow to gain additional information about the neutrino mass matrix and in particular it could solve the ambiguity on the sign of Δm.

For all the above reasons it is very important to compare the behaviour of neutrinos and antineutrinos. The use of neutrino and antineutrino beams can help in reducing the effect of the theoretical uncertainties (on the non–oscillated flux and on neutrino cross sections) in the determination of the oscillation parameters.

The currents in the NGS horn and reflector can easily be inversed to focus the negatively charged parent mesons, and defocus the positive, so as to produce an $\overline{\nu}_\mu$ beam. The neutrino channel is favoured both in production and in interaction cross section at the detector. The $\overline{\nu}_\mu$ flux obtained is therefore some 75% of that in the ν_μ beam, and the CC event rate is about 35%: in a preliminary simulation, 200 $\overline{\nu}_\mu$ CC events per kiloton of detector and per 10^{19} pot have been obtained in the energy interval 0-100 GeV. Calculated fluence and event spectra are given in Fig. 12.

More significantly, the ν_μ and ν_e backgrounds in the $\overline{\nu}_\mu$ beam are a factor of 10 higher in the anti-neutrino beam than the equivalent backgrounds in the neutrino beam. It should be possible to reduce these backgrounds by some 30%, at the expense of a small loss in $\overline{\nu}_\mu$ flux, by installing an axial absorber after the target: parameters of such an absorber are under study.

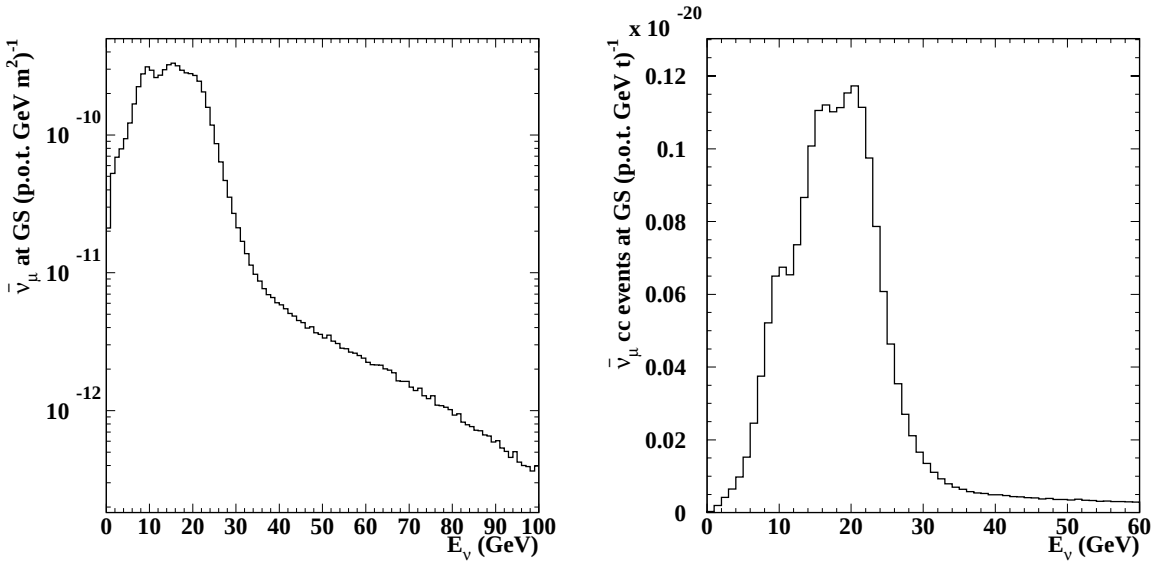

Figure 12: *Energy distribution of the $\overline{\nu}_\mu$ fluence (left) and of the CC $\overline{\nu}_\mu$ interactions (right) at Gran Sasso (preliminary results).*

4 Radiological Aspects

Estimates of the radiological parameters of concern for the environment and facility maintenance are in the process of being revised according to the new reference parameters. The new shielding around the horn, decay tube etc. already takes account of the need to reduce doses received by personnel maintaining these components. The extra shielding also keeps the radioactivity induced in the air and the rock outside the target cavern per proton on target to values lower than those achieved in the 1998 study. However the present project suggests that the upper limit of the number of protons on target could be up to 50% higher than before. This upper limit would be reached if the NGS beam were to run in dedicated mode (no other SPS users). Long-lived radioactivity levels will be correspondingly higher. Optimization studies are continuing.

5 Update on the NGS schedule

The schedule shown in Fig. 13 assumes that the approval of the NGS facility is granted no later than December '99. Then the call for tender for civil engineering work can be launched immediately - drawings are readily available -, so that the civil works can start effectively in October 2000. These nine months will also be used to obtain all necessary authorisations from the CERN Host States.

Thirty months are needed for completing all civil engineering works shown in the first part of the schedule. It should be stressed that this time span is a bare minimum and that there is no margin for unforeseen problems. Moreover, the assumed speed for the tunnel boring machine is higher than the one anticipated for boring TI8, although the negative slope is larger for NGS.

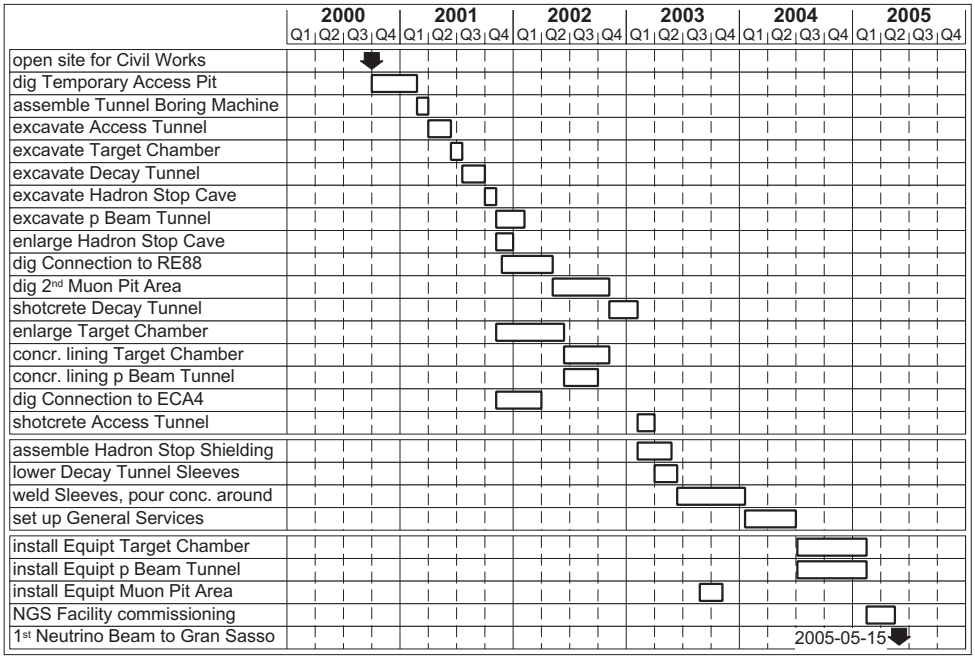

Figure 13: *Present construction schedule of the NGS beam project.*

If such a speed can be met, interference with LHC work and SPS winter shutdowns can be avoided.

The second step concerns the construction of the hadron stop and of the decay tunnel pipe, as well as the setting up of general services, for an overall time span of 18 months. The last step concerns the installations in the target cave and of the proton beam line, for which 9 months are a strict minimum. These two steps are somewhat longer than in the NGS report [2]: more detailed studies have shown that some installation work cannot be done in parallel and that more time in the target cave is needed. Studies are being carried out to see if it is possible to shorten these last two steps, without reducing NGS performance, but this may become interesting only if more than 6 months could be gained, in order to be able to commission NGS before the SPS winter shutdown at the end of 2004. As a final remark, it must be recalled that the time between NGS approval and NGS commissioning is not constant but may have to be increased if the NGS approval is delayed, as some operations must be done during accelerator winter shutdowns and constraints by the LHC schedule have to be respected.

A Updated Reference Parameter List - May 1999

Proton Beam

Maximum proton beam momentum (design)	450 GeV/c
Proton beam momentum (assumed for operation)	400 GeV/c
Proton beam normalised emittance (1σ)	12π mm mrad
β^* at the focus (H and V)	2.5 m
$\rightarrow$ minimum beam size / maximum divergence (1σ)	0.27 mm, 0.1 mrad
Minimum repetition time (dedicated operation at 400 GeV/c)	6 s
Time between bursts	50 ms
Proton intensity (for hadron stop considerations)	6×10^{12} protons/second, 200 days/year
Proton intensity (for environmental considerations)	7.6×10^{19} protons/year
Expected integrated number of protons per year at 400 GeV/c	4.5×10^{19} protons
Expected period of operation	10 years

Target Chamber

Length of target chamber	115 m
Diameter of target chamber	6.5 m (int.)
Floor width of target chamber	5.6 m
Enlargement at target (optional)	7.4 m
Crane capacity	10 t
Free height under crane hook	3.7 m
Beam height in target chamber	1.6 m
Diameter of neutrino service gallery	3.4 m (int.)
Distance of service gallery from cavern	6.0 m
Length of junction tunnel to target chamber	8 m
Distance of proton focus to entrance of decay tunnel	100 m

Target

Start coordinate (w.r.t. proton focus)	-0.5 m
End coordinate (w.r.t. proton focus)	$+1.5$ m
Target material	carbon, density 1.81 g/cm^3
Target rod length	10 cm
Diameter of rods	4 mm
Number of rods	13
Distance between rods	first 8 rods with 9 cm distance, last 5 rods minimal possible distance

Note: the exact configuration of the 13 target rods is under investigation.

Helium tubes

Helium tube I

Start coordinate (w.r.t. proton focus)	11.00 m
End coordinate (w.r.t. proton focus)	42.00 m
Diameter first 6 m	0.80 m
Diameter remaining length	1.20 m

Helium tube II

Start coordinate (w.r.t. proton focus)	52.00 m
End coordinate (w.r.t. proton focus)	99.00 m
Diameter	1.20 m

Shielding / Collimation

Shielding 1 (around the target, cf. Fig 7)

Material	iron / marble
Start coordinate (w.r.t. proton focus)	-1.5 m
End coordinate (w.r.t. proton focus)	$+1.7$ m
Cross-section	rectangular
Opening for target box	60×60 cm^2
30 cm of marble added at downstream end of target	

Shielding 2 (around the horn, cf. Fig 7)

Shielding underneath the horn	40 cm concrete
Side walls of 30 cm marble / 20 cm iron / 30 cm concrete	
Height of walls	3.20 m
Left wall, start coordinate (w.r.t. proton focus)	2.30 m
Left wall, end coordinate	10.80 m
Right wall, start coordinate	2.00 m
Right wall, end coordinate	11.00 m

Shielding 3 (around helium tube I, cf. Fig 6)

Upstream shielding	0.50 m marble
Shielding collar, first 5 m	iron, 3×3 m^2
	opening 0.80×0.80 m^2
Shielding collar, remaining 25.5 m	0.20 m iron, 0.30 m concrete
	opening 1.20×1.20 m^2
(Height of collar 2.70 m)	

Shielding 4 (along helium tube II, cf. Fig 6)

Shielding underneath the tube	0.40 m concrete
Side walls height	3.20 m

Left wall distance to axis	1.00 m
Left wall thickness	0.80 m
Right wall distance to axis	1.00 m
Right wall thickness	0.80 m

Shielding 5 (collimator around helium tube II, cf. Fig 6)

Start of shielding	85 m
Length of shielding	5 m
Inner diameter	1.20 m
Outer diameter	3.80 m (exception: downwards)

Horn and Reflector (dimensions referring to **magnetic length**):

Distance proton beam focus - horn entrance	1.7 m
Length of horn	6.65 m
Current in horn	150 kA
Distance proton beam focus - reflector entrance	43.35 m
Length of reflector	6.65 m
Current in reflector	150 kA

Note: for the beam calculations, it is assumed that all spaces outside the horn and reflector are filled with helium at 1 atm.

Decay Tunnel

Upstream end of decay tunnel (w.r.t. focus)	100 m
Length of decay tunnel	992 m
Diameter of decay tunnel (TBM)	3.50 m (ext.)
Length of decay pipe	994.5 m
Diameter of decay pipe (inner diam. steel pipe)	2.45 m (96 inch)
Wall thickness decay pipe	16 - 19 - 22 mm
Concrete filling around pipe	ca. 53 cm
Entrance window decay pipe	diameter 1.40 m, 2 mm titanium T40
Protecting shutter (thickness)	3 cm steel
Exit window decay pipe	5 cm steel
Pressure in decay pipe (min.)	1-2 Torr
Pumping down time (max.)	2 weeks

Hadron Stop and Muon Chambers

Upstream end of hadron stop cavern (w.r.t. proton focus)	$100 + 992\,\mathrm{m}$
Length of hadron stop cavern	$26\,\mathrm{m}$
Diameter of hadron stop cavern	$6\,\mathrm{m}$ (int.)
Length of hadron stop	$18.2\,\mathrm{m}$
Cross-section of hadron stop	$4 \times 4\,\mathrm{m}^2$
Length of graphite insert	$3\,\mathrm{m}$
Cross-section of graphite insert	$2.6 \times 2.6\,\mathrm{m}^2$
Wall thickness of aluminium box around graphite	$0.1\,\mathrm{m}$
Length of airgap upstream of hadron stop	$0.25\,\mathrm{m}$
Length of airgap downstream of hadron stop	$5\,\mathrm{m}$
(= length of first muon chamber)	
Length of “muon filter”: Molasse	$67\,\mathrm{m}$
Length of 2nd muon chamber	$3.5\,\mathrm{m}$
Muon pit “service alcove” surface	$10 \times 4\,\mathrm{m}^2$
Access gallery to hadron stop: diameter	$3.1\,\mathrm{m}$ (int.)
Access gallery to 2nd muon pit: diameter	$2.5\,\mathrm{m}$ (int.)

B Isometric drawings of the target chamber

The following drawings are deduced from the information on geometry and material used in the FLUKA98 calculations of the radiological issues concerning NGS. The drawings are produced using AUTOCAD - the help of Helmut Vincke (EP/ATI) is acknowledged.

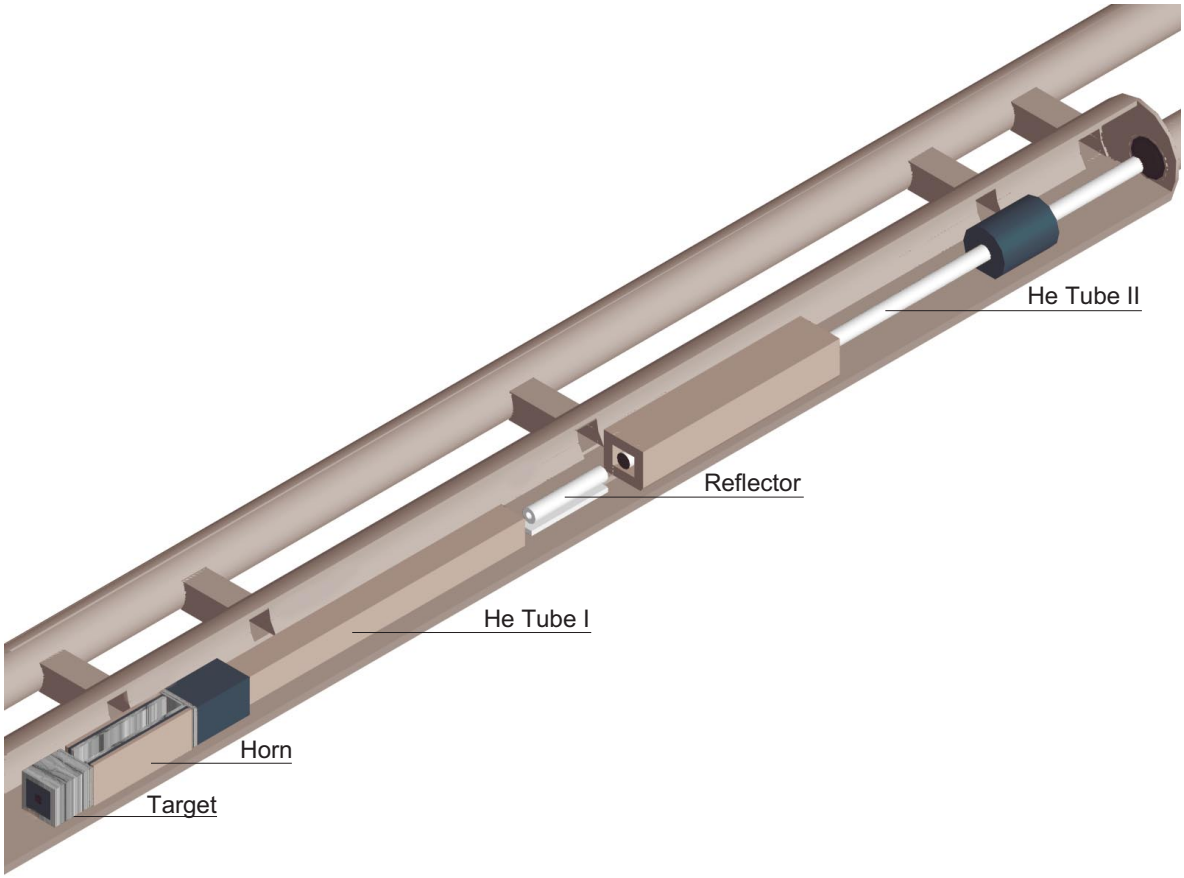

Figure 14: *View into the target chamber with NGS beam components and shielding. The service gallery parallel to the target chamber and the various connecting alcoves are also shown.*

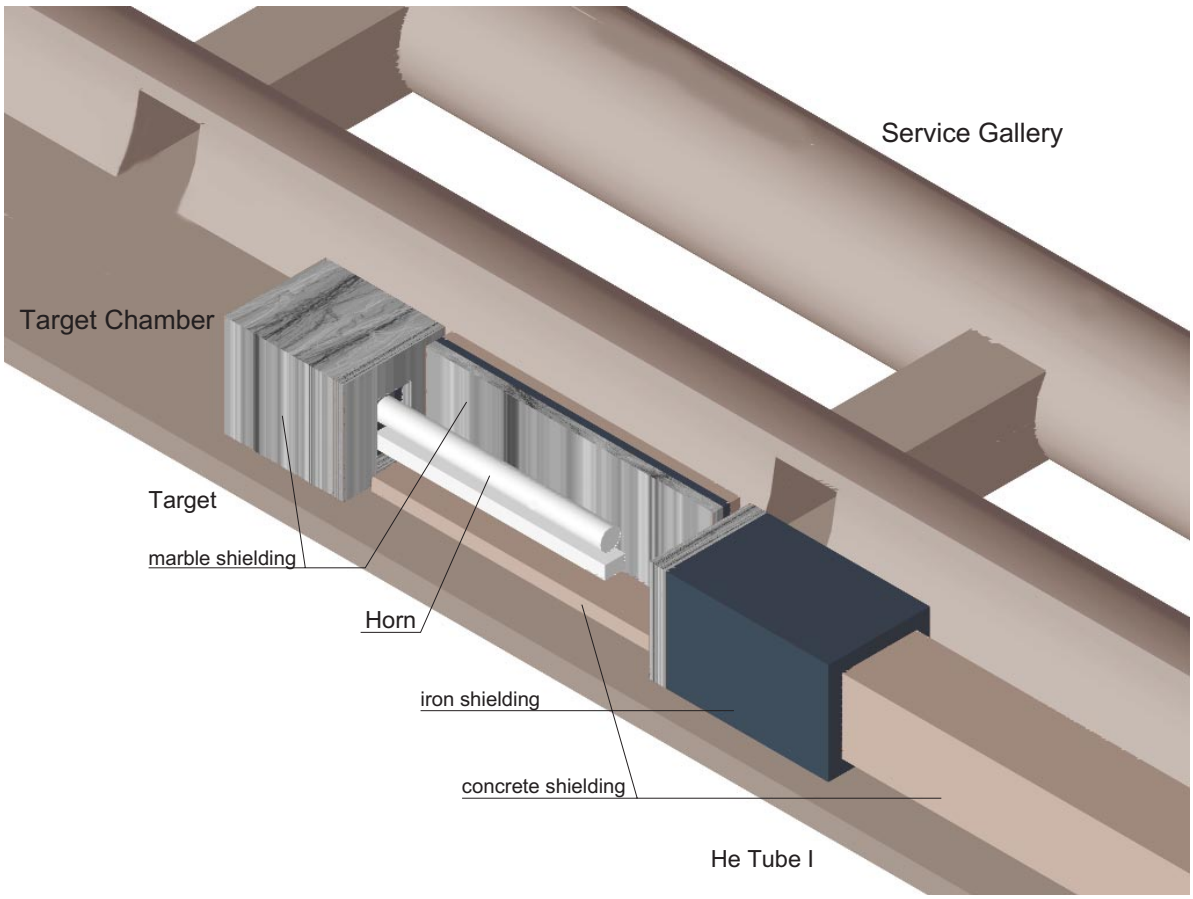

Figure 15: *Details of the target/horn region. One shielding wall on the side of the horn is removed, for better insight.*

C Design of horn and reflector for the new NGS reference beam

Details of the new design of horn and reflector are summarised in this Appendix. The co-ordinates of the inner and outer conductors, as used in the simulations of the new NGS reference beam, are given in Table 7. The cross sections corresponding to this design are shown in Fig. 16. Finally, an updated table of the electrical characteristics of the new horn and reflector is shown as Fig. 17 - this takes into account the higher current of the focusing elements and includes corrected values of the inductances and resistances.

Table 7: *Horn and reflector current line and conductor coordinates.*

	HORN		REFLECTOR	
Current	150 kA		150 kA	
Start coordinate	1.70 m		43.35 m	
Length	6.65 m		46.65 m	
Inner conductor	L [cm]	R_I [cm]	L [cm]	R_I [cm]
	0.0	3.900	0.0	26.56
	106.0	5.060	338.9	19.27
	175.1	5.535	517.3	13.20
	250.0	5.920	581.4	10.00
	329.1	5.990	665.0	10.00
	409.8	5.800		
	449.5	5.580		
	488.0	5.260		
	524.6	4.860		
	558.5	4.370		
	589.0	3.790		
	615.2	3.140		
	636.5	2.420		
	652.2	1.640		
	662.5	0.730		
	665.0	0.730		
Outer conductor	L [cm]	R_I [cm]	L [cm]	R_I [cm]
	665	30.0	665	60.0

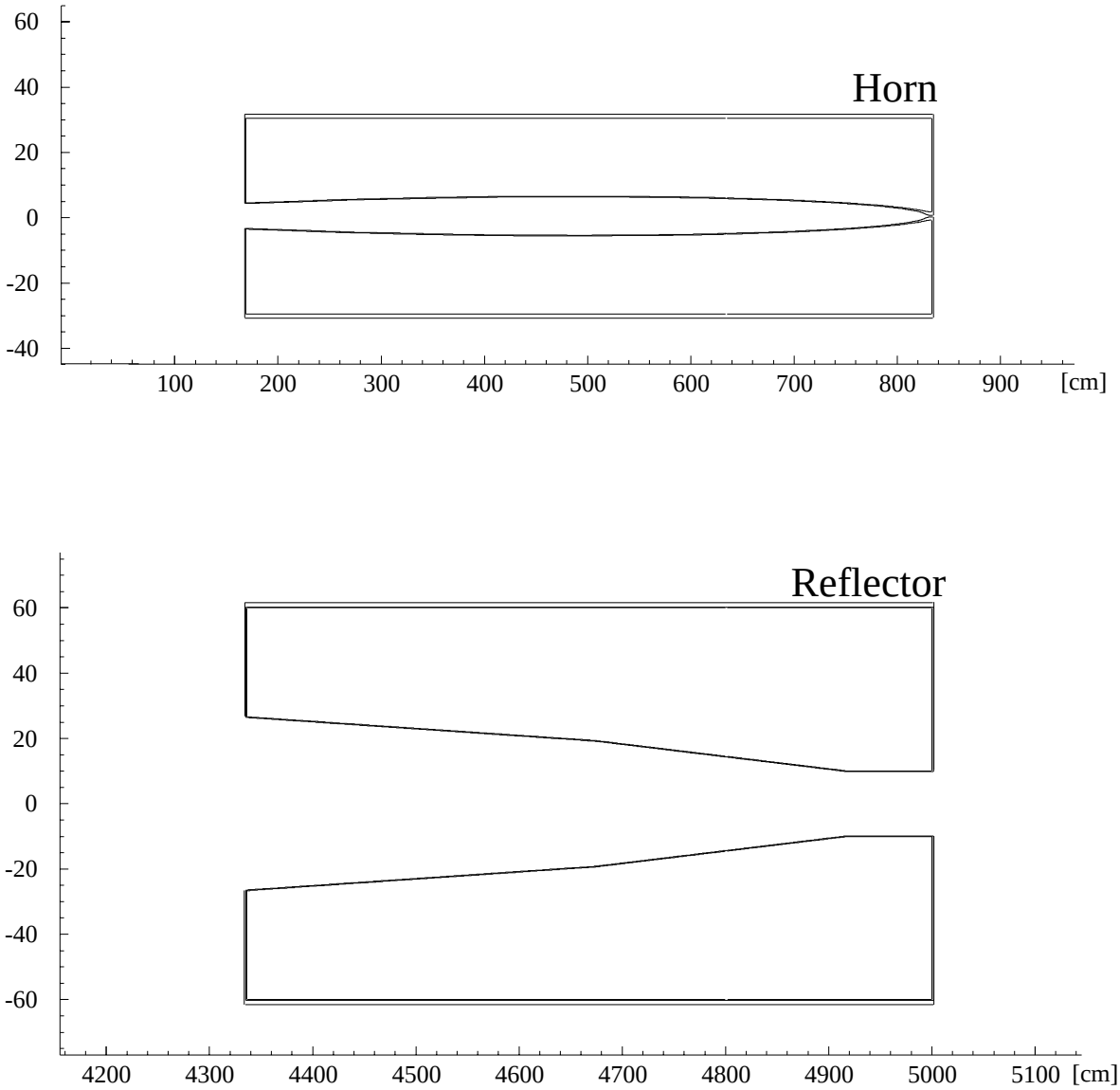

Figure 16: *Cross section of the conductor in horn and reflector.*

	HORN SYSTEM		REFLECTOR SYSTEM	
Peak current in element	150 kA		150 kA	
Transformer ratio	16		16	
Primary current peak	9375 A		9375 A	
Inductance element	2.15 µH x 16^2	0.55 mH	1.17 µH x 16^2	0.30 mH
connections	0.12 µH x 16^2	0.03 mH	0.12 µH x 16^2	0.03 mH
striplines (30 m length)	20 nH x30x 16^2	0.15 mH	20 nH x30x 16^2	0.15 mH
transformer		0.04 mH		0.04 mH
cable (800m) 240 mm^2		0.013 mH		0.013 mH
TOTAL		0.79 mH		0.54 mH
Resistance element	0.405 mΩ x 16^2	0.104 Ω	0.33 mΩ x 16^2	0.051 Ω
striplines (30 m length)	2.5 µΩ x30 x 16^2	0.019 Ω		0.019 Ω
transformer		0.020 Ω		0.020 Ω
cable (800m) 630 mm^2 Al		0.080 Ω		0.080 Ω
TOTAL		0.223 Ω		0.170 Ω
Total capacitance for one switching section	45.4 µF x 50	2270 µF	45.4 µF x 30	1362 µF
Pulse duration		4.3 ms		2.7 ms
charging voltage		7210 V		7170 V
voltage on element		450 V		448 V
Duty cycle	2 pulses 50ms apart all 6 s		2 pulses 50ms apart all 6 s	
r.m.s. current in element		4008 A		3192 A
mean power dissipation in element by current only*		6422 w		2014 w
r.m.s. current in cable		250 A		199 A
r.m.s. current density in cable	0.40 A / mm^2		0.32 A / mm^2	
max. voltage drop in cable		751 V		751 V
mean power dissipation in cable		5020 w (6.3 w / m)		3184 w (4.0 w / m)

* power dissipation due to beam absorption has to be added

Figure 17: *Electrical characteristics of horn and reflector (replaces Table E.1. in [2]).*

D Normalised representation of material for all NGS calculations

The normalised material representation used in beam optics evaluations for the new NGS reference beam is given, taking into account the recent developments:

- change in the target layout to incorporate more material in the 2 m length available
- increase in the current to 150 kA in horn and reflector
- re-evaluation of thicknesses of conductors and support structures in horn and reflector
- beam collimators, as given in Appendix A.

D.1 Tunnel representation

The general description and dimensions are given in the reference parameter list, Appendix A. The system origin (Z_0) is the nominal focal point of the proton beam. The target chamber volume, from the front of the target to the decay tunnel window at Z = 100 metres is assumed to be filled with helium gas at NTP, except for the volumes of the horn and reflector, which are assumed to contain air at NTP. The entrance window to the decay pipe is titanium of 2 mm thickness. The length of the evacuated decay tunnel is assumed to be 1000 m, it ends at Z = 1100 metres.

D.2 Target representation

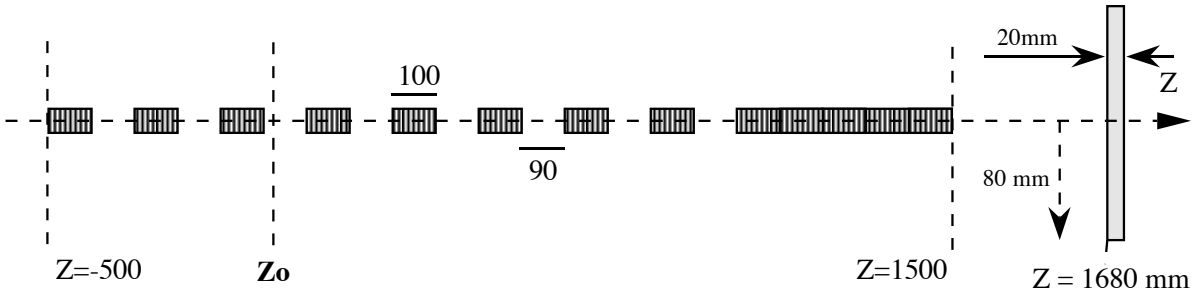

Figure 18: *Schematic view of the target representation used in the NGS simulations.*

The nominal focal point of the proton beam Z_0 is also the origin of the secondary beam focusing system.

The target consists, for the purpose of the simulations, of 8 rods of 100 mm length, separated by gaps of 90 mm, with a final rod of 480 mm length - this approximates the target material in 13 rods of 100 mm each. The radius of the rods is 2 mm. The material is carbon with density 1.81 g/cm^3. The target starts at at -500 mm and ends at 1500 mm with respect to Z_0.

The support structures of the target rods are simulated by an aluminium plate of 20 mm thickness and 80 mm radius, starting at Z = 1680 mm. All surrounding volumes are assumed to be filled with He gas at NTP.

D.3 Beam collimators representation

Two collimators are considered as thick walled steel cylinders, co-axial with the beam axis:

- **Collimator 1**, approximating Shielding 3: starting at $Z = 11.5$ m, ending at $Z = 16.5$ m; inner radius 450 mm, outer radius 1700 mm (note that these are the equivalent to the square inner cross section of $0.8 \times 0.8\,\mathrm{m}^2$ and the square outer cross section of $3 \times 3\,\mathrm{m}^2$).
- **Collimator 2**, approximating Shielding 5: starting at $Z = 85$ m, ending at $Z = 90$ m; inner radius 600 mm, outer radius 1900 mm.

Other components of the shielding, as shown in Appendices B and A, are not limiting the apertures and are therefore not considered as beam-line elements in the simulations.

D.4 Horn and Reflector representation

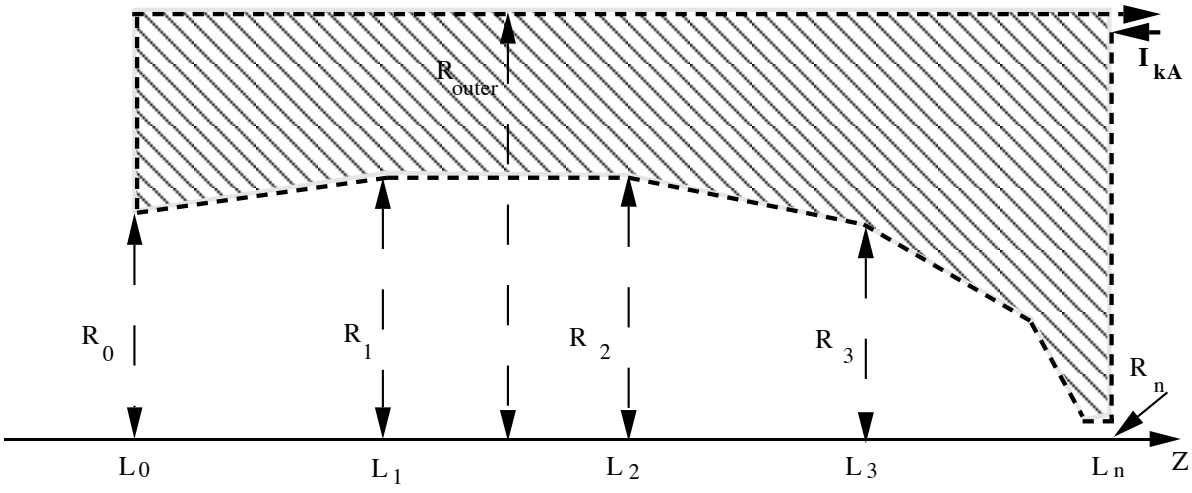

Figure 19: *Horn and reflector conductors used in the NGS simulations.*

The magnetic field region is defind as being between co-axial inner and outer conductor sheets with the field at any point given by B[T] = 0.2 × I[kA] / R[mm]. The inner conductor is assumed to be a set of joined frusta with radial coordinates R(0,n) at Z-coordinates L(0,n). The outer conductor is assumed to be cylindrical with a constant radius R(outer). The current is set to 150 kA. The magnetic length [L_n - L_0] should not exceed 6650 mm. The field is radially symmetric about the beam axis (Z). There is no field before L_0 or after L_n, inside the inner conductor or outside of the outer conductor.

All material in the horn and reflector is aluminum except a support disk which simulates the equivalent thickness of the steel tension wires: other spaces are assumed to be air at NTP. The material thicknesses of the inner conductor are given by a 'half-thickness' t so that the inner radius of the inner conductor is (R - t) and the outer radius of the outer conductor is (R + t) at the beginning and end of each frustrum.

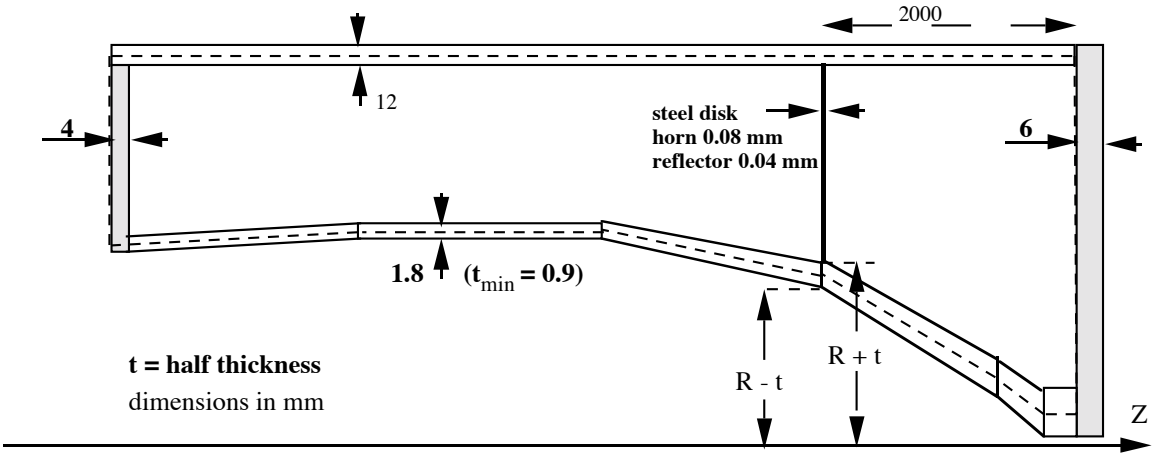

Figure 20: *Material thicknesses in horn and reflector, as used in the NGS simulations.*

For 150 kA and 1 ms curent pulse. t[mm] can be calculated as $t = 490 / (4 \times \pi \times R[\text{mm}])$. The minimum thickness is 1.8 mm ($t = 0.9$ mm). The outer conductor has a half-thickness of 6 mm.

The end plates and internal support structures, orthogonal to the beam direction, are defined as:

- Front plate: start L_0, end $L_0 + 4$ mm; inner radius $R_0 + t$, outer radius R(outer) - 6 mm.
- Support disk: horn 0.08 mm thick steel, reflector 0.04 mm thick steel (density 7.5 g/cm^3), located at L_n - 2000 mm; inner radius $R + t$, outer radius R(outer) - 6 mm.
- Rear plate: start L_n. emd $L_n + 6$ mm; inner radius $R_n - t$, outer radius R(outer) + 6 mm.

E Errata in report CERN 98-02 / INFN-AE/98-05

The following errors in the NGS report [2] have been pointed out to us:

page 29, footnote:
The losses of ν_τ CC events at Gran Sasso due to 1 atm of air instead of vacuum in the decay pipe would be about 28%, for 1 atm of Helium the losses amount to about 7%.

page 33, bottom of page:
The slope of the cross section should read 0.67×10^{-38} cm^2/GeV.

References

[1] Y. Fukuda $et\ al.$, Phys. Rev. Lett. **81** (1998) 1562.

[2] G. Acquistapace et al. The CERN Neutrino Beam to Gran Sasso, Report CERN 98-02 and INFN/AE-98/05.

[3] The NGS beam optics working group, *Progress on NGS beam studies*, memorandum CERN/SPSC/98-35.

[4] *Decisions taken at the 40th SPSC meeting on 3-4 November 1998*, CERN/SPSC 98-41, 20 November 1998.

[5] A.E. Ball et al., *The CERN Neutrino Beam to Gran Sasso, An updated summary*, CERN/AC Note (99-01).

[6] M.Colin, G. Cultrut and B. Desforges, D. Picard, *1997 SPS and LEP Machine Statistics*, CERN SL-Note-98-068 OP.

[7] The LHC Study Group, *The Large Hadron Collider*, CERN/AC/95-05(LHC).

[8] The SLI (SPS as LHC injector) WWW page: http://nicewww.cern.ch/sl/sli/Sli.html

[9] P. Ciriani, S. Claudet, A. Faugier, K. Hubner, S. Myers, P. Sphicas, E. Tsesmelis, *CERN Energy Budget and Accelerator Schedules*, CERN/AC Note (98-01).

[10] E. Weisse, *The CERN neutrino beam to Gran Sasso (NGS)*, Proc. Workshop on LEP-SPS, Chamonix IX, 25-29 January 1999, ed. J. Poole, CERN-SL/99-007(DI), p. 36-40.

[11] G. Baum et al., COMPASS Add.1, SPSLC/96-30/P297/Add.1 (20.5.96).

[12] The NGS WWW-page: http://www.cern.ch/NGS

[13] G. Collazuol et al., *Neutrino beams: production models and experimental data*, preprint CERN-OPEN-98-32, submitted to Nucl. Inst. Meth. A.

[14] The CERN program library.

[15] P. Lipari, *Matter effects in long baseline experiments, the flavor content of the heaviest (or lightest) neutrino and the sign of* Δm^2, preprint HEP–PH 9903481 (1999).

[16] G. Fiorentini and B. Ricci, *Old and New Interactions in Long baseline Neutrino Experiments*, INFN Ferrara 06-93, Proc. of Workshop on Neutrino Telescopes, Venice, March 1993, ed. M. Baldo-Ceolin.